

Synthesis and Properties of Boron(III)-Coordinated Subbacteriochlorins

Shin-ya Hayashi,[†] Eiji Tsurumaki,[†] Yasuhide Inokuma,[†] Pyosang Kim,[§] Young Mo Sung,[§] Dongho Kim,^{*,§} and Atsuhiko Osuka^{*,†}

[†]Department of Chemistry, Graduate School of Science, Kyoto University, Sakyo-ku, Kyoto 606-8502, Japan

[§]Spectroscopy Laboratory for Functional π -Electronic Systems and Department of Chemistry, Yonsei University, Seoul 120-749, Korea

S Supporting Information

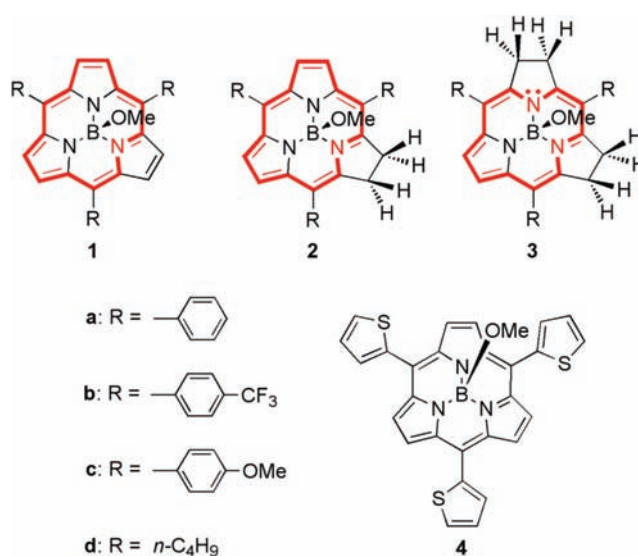
ABSTRACT: Subbacteriochlorins, which were prepared via hydrogenation of subporphyrins with Raney nickel, are modestly aromatic due to 14π -diazannulenic circuit and exhibit characteristic blue-shifted Soret-like bands, intensified fluorescence spectra, and high oxidation potentials.

Doubly reduced porphyrins such as bacteriochlorins and isobacteriochlorins play vital roles in natural systems. Bacteriochlorophylls are photosynthetic pigments which had been used before the emergence of chlorophylls and are still around in purple bacteria and other anaerobic or microaerobic bacteria.¹ Sirohydrochlorin, having an isobacteriochlorin framework, serves as a redox enzyme and a biosynthetic intermediate of vitamin B₁₂.² These macrocycles retain 18π -conjugated circuits, while displaying attenuated Soret bands and low-energy lying and intensified Q-bands as compared with porphyrins because of changes in the molecular orbital diagrams. Various synthetic bacteriochlorin models have been explored to understand and examine their unique optical and electronic properties.³

In recent years, subporphyrin has emerged as a genuine ring-contracted porphyrin that bears a 14π -electronic circuit lying on a curved bowl-shaped conformation.^{4,5} While sharing some attributes with porphyrins, *meso*-aryl-substituted subporphyrins exhibit extremely substituent-dependent optical properties due to effective conjugative interactions of the subporphyrin core with *meso*-aryl substituents, which arise from their small rotational barriers.⁶ Subchlorins, singly reduced subporphyrins, were recently prepared by reduction of subporphyrins with *p*-tosylhydrazide under basic conditions.⁷ Optical and electrochemical properties of subchlorins change from those of subporphyrins in an analogous manner to the changes from porphyrins to chlorins. As shown in Chart 1, while subporphyrins **1** and subchlorins **2** share [14]azaannulene circuits and are aromatic, subbacteriochlorins **3** have a rare [13]diazannulene circuit, in which the 14π -electronic conjugation is kept through the lone-pair electrons of the nitrogen atom.⁸

Here we report the first synthesis of subbacteriochlorins. Raney nickel was found effective for hydrogenation of *meso*-substituted subporphyrins **1a–c** to furnish *meso*-aryl-substituted subbacteriochlorins **3a–c** in 47, 21, and 39% yields, respectively. The reduction of **1a** and **1b** was conducted in THF at 60 °C, while **1c** was reduced at 40 °C to suppress the degradation of **3c**.

Chart 1. Subporphyrin **1** and **4**, Subchlorin **2**, and Subbacteriochlorin **3**; 14π -Electronic Circuits Are Indicated in Red Bold Lines



meso-Alkyl-substituted subbacteriochlorin **3d** was prepared in 16% yield by the reduction of *meso*-(2-thienyl)-substituted subporphyrin **4**, since subporphyrin **1d** was formed from **4** under these reduction conditions.^{9,10} Here it is worthy to note that any further reduction over subbacteriochlorin has not been detected for all the cases, and quick separation over a silica gel column is critical for the isolation of pure subbacteriochlorins due to their feasibility toward oxidation. The high-resolution electrospray ionization mass measurement revealed intense borenium cation peaks at m/z 474.2140 (calcd for C₃₃H₂₅B₁N₃ = 474.2142 [**3a** – OMe]⁺), m/z 678.1766 (calcd for C₃₆H₂₂B₁N₃F₉ = 678.1764 [**3b** – OMe]⁺), m/z 564.2464 (calcd for C₃₆H₃₁B₁N₃O₃ = 564.2459 [**3c** – OMe]⁺), and a cationic parent peak as a B-axial hydroxy derivative at m/z 431.3094 (calcd for C₂₇H₃₈B₁N₃O₁ = 431.3107 [**3d** – OH]⁺). The ¹H NMR spectrum of **3a** in CDCl₃ exhibits a singlet at 6.87 ppm due to the β -pyrrolic protons and four signals at 3.68, 3.41, 3.21, and 3.12 ppm due to the saturated methylene β -protons that correlate to each other. The B-axial methoxy protons resonate at 2.34 ppm, which is slightly

Received: January 23, 2011

Published: March 07, 2011

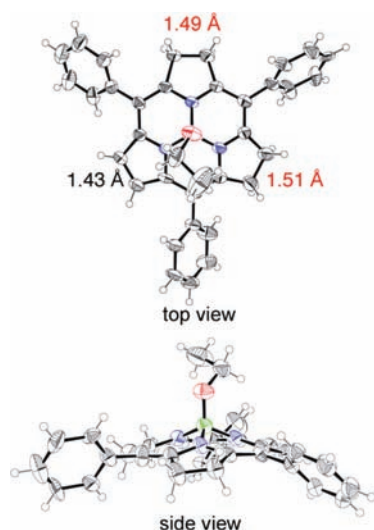


Figure 1. X-ray crystal structure of **3a-OEt**. Thermal ellipsoids represent 50% probability. Solvent molecules are omitted for clarity.

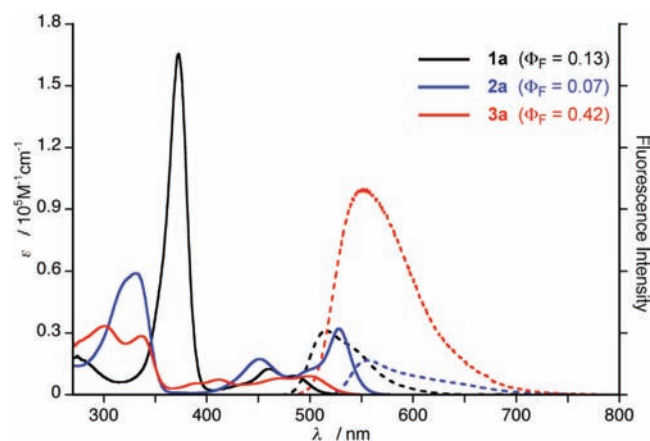


Figure 2. UV-vis absorption (solid lines) and fluorescence (dashed lines) spectra of **1a**, **2a**, and **3a** in CH_2Cl_2 .

downfield shifted from those of **1a** (0.82 ppm) and **2a** (1.51 ppm), and the central boron resonates at -8.0 ppm that is also downfield shifted from those of **1a** (-15.3 ppm) and **2a** (-12.2 ppm). These data indicate distinct aromaticity of **3a**, which is modest as compared with those of **1a** and **2a**. In line with this trend, the nuclear independent chemical shifts (NICS) value of **3a** has been calculated at B3LYP/6-311G(d) level using the Gaussian 09 package¹¹ to be -10.9 ppm, which is again smaller than those of **1a** (-18.9 ppm) and **2a** (-14.9 ppm).

Slow recrystallization from a mixture of acetonitrile and heptane provided nice crystals of **3a-OEt** that was easily prepared by heating **3a** in the presence of ethanol. Single-crystal X-ray diffraction analysis revealed that **3a-OEt** has a nonsymmetric structure with two β – β single bonds of 1.486(5) and 1.511(5) Å and a β = β double bond of 1.425(5) Å and a bowl-depth of 1.26 Å¹² (Figure 1).

Figure 2 shows the absorption and emission spectra of **1a**, **2a**, and **3a**. The absorption spectrum of subchlorin **2a** is characterized by an attenuated and blue-shifted Soret-like band as well as intensified and red-shifted Q-like bands as compared to those of

subporphyrin **1a**.⁷ Subbacteriochlorin **3a** exhibits even smaller and double-peaked Soret-like bands at 301 and 336 nm and Q-like bands at 393, 412, 472, and 498 nm. Importantly, the fluorescence of **3a** is remarkably intensified ($\Phi_F = 0.42$) at 550 nm, which is distinctly red-shifted from **1a** (520 nm, $\Phi_F = 0.13$) or slightly blue-shifted from **2a** (556 nm, $\Phi_F = 0.07$). These spectral changes are reminiscent of those from chlorins to isobacteriochlorins rather than to bacteriochlorins.¹³ Notable substituent effects are observed for the Soret bands of subbacteriochlorins; the similar double-peaked Soret band is observed for **3c**, a single-peaked Soret band is observed for **3b**, and a much sharper Soret band is observed for **3d** due to the absence of conjugative electronic interaction with *meso*-substituent, while the substituent effects are marginal for the fluorescence spectra (Figure S4, Supporting Information [SI]).

To quantitatively analyze the energy relaxation dynamics of **3a** in the S_1 state, the radiative and nonradiative decay rates have been determined using the fluorescence quantum yield and the S_1 fluorescence lifetime (Table S2, SI). Since the nonradiative decay rates of subporphyrin and subchlorin are nearly 10 times faster than their radiative decay rates presumably due to an efficient intersystem crossing process,^{6a,7} the overall S_1 fluorescence lifetimes of these molecules are mainly determined by the nonradiative decay rates. In the case of **3a**, however, the nonradiative decay rate ($9.8 \times 10^7 \text{ s}^{-1}$) was similar to the radiative decay rate ($6.6 \times 10^7 \text{ s}^{-1}$) probably by decreasing the intersystem-crossing rate, which leads to an increased fluorescence quantum yield. On the other hand, the nonradiative decay rates of **1a** and **2a** were estimated to be $4.4 \times 10^8 \text{ s}^{-1}$ and $3.2 \times 10^8 \text{ s}^{-1}$, respectively. The reason for slower intersystem crossing in **3a** is probably a lowered energy level of its triplet state which can lead to an increased energy gap between the singlet and triplet states as compared to those of subporphyrins and subchlorins. Further support for this conjecture comes from a triplet state lifetime of **3a** (30 μs) that is shorter than those of **1a** (60 μs) and **2a** (100 μs), which have been determined by nanosecond time-resolved transient absorption spectra (Figure S9, SI). These data are consistent with a decrease in the fluorescence quantum yield in the order of **3a** > **1a** > **2a**.

The molecular structures and MO diagrams were optimized at B3LYP/6-311G(d) level using the Gaussian 09 package (Figure 3).¹¹ The molecular orbitals of subporphyrin **1a** are similar to those of porphyrin in terms of a_{2u} -like HOMO, a_{1u} -like HOMO-1, and a couple of degenerate e_g -like LUMO and LUMO+1. Subchlorin **2a** possesses destabilized a_{1u} -like HOMO and largely destabilized LUMO+1 along with HOMO-1 and LUMO that are lying at energy levels similar to those of **1a**. Upon another β -hydrogenation, the LUMO and LUMO+1 of **3a** are stabilized and destabilized, respectively, to become LUMO+1 and LUMO, and HOMO are further destabilized. This MO diagram can explain two-peaked Soret band features of **3a** and **3c** on the basis of Gouterman's four orbital model.¹⁴ In **3b**, the electron-withdrawing 4-trifluoromethylphenyl substituents considerably stabilize LUMO+1, hence making the energy gap between LUMO and LUMO+1 small, which causes a single-peaked Soret-like band.

The electrochemical properties of **3a–d** were studied by the cyclic voltammetry in CH_3CN containing 0.10 M Bu_4NPF_6 as a supporting electrolyte (Figure S5, SI). Subbacteriochlorins **3a–d** exhibit irreversible reduction waves with peak positions at -2.53 , -2.33 , -2.53 , and -2.82 V, respectively, and quasi-reversible oxidation waves at 0.00 and 0.57 V, and 0.06 and 0.63 V,

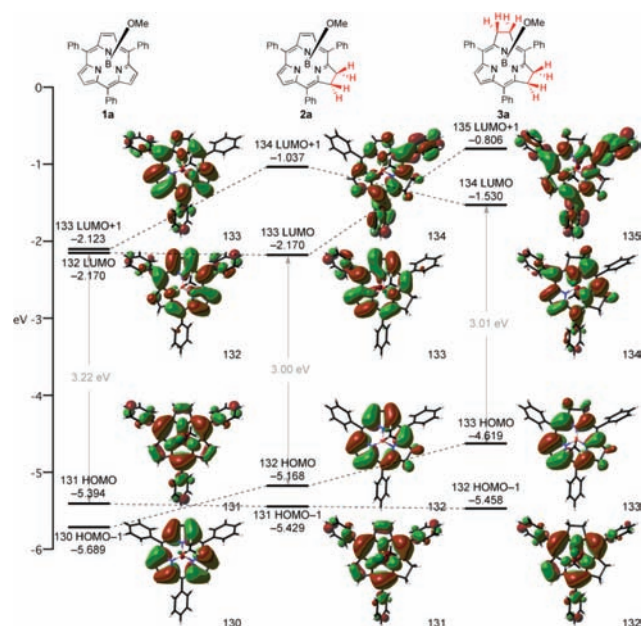


Figure 3. MO diagrams of **1a**, **2a**, and **3a** calculated with Gaussian 09 package.¹¹ (All energy levels were calculated at the B3LYP/6-311G(d) level. And each MO was visualized with cubegen program.)

−0.05 and 0.43 V, and −0.18 and 0.35 V, respectively. Characteristically high oxidation potentials of subbacteriochlorins are in accord with their easily oxidizable propensity with molecular oxygen.

Finally, **3a** was found to be smoothly and selectively oxidized to **2a** with Ag_2O in 86% yield. Therefore, the initial reduction of subporphyrin to subbacteriochlorin followed by oxidation with Ag_2O constitutes a novel synthetic route to subchlorins that is superior to our previous direct route of the reduction of **1** with *p*-tosylhydrazide.⁷ Actually, subchlorin **2a** was prepared in 74% from **1a** via the two-step route involving the Raney nickel reduction and the Ag_2O oxidation without isolation of unstable **3a**.

In summary, subbacteriochlorins were synthesized by the hydrogenation of subporphyrins with Raney nickel. Despite double β -hydrogenation, subbacteriochlorins are modestly aromatic owing to the 14π -electronic circuit that involves the lone pair electrons of the nitrogen atom and exhibit characteristic blue-shifted Soret-like bands, red-shifted Q_2 -like bands, enhanced fluorescence, and high oxidation potentials. Incorporation of this interesting porphyrinic chromophore into novel functional molecular systems is now actively pursued in our laboratories.

■ ASSOCIATED CONTENT

Supporting Information. Preparation and analytical data for samples, crystallographic data for **3a-OEt** (CIF), cyclic voltammograms, calculated molecular orbitals, and time-resolved fluorescence decays and nanosecond time-resolved transient absorption decays. Complete ref 11. This material is available free of charge via the Internet at <http://pubs.acs.org>.

■ AUTHOR INFORMATION

Corresponding Author

dongho@yonsei.ac.kr; osuka@kuchem.kyoto-u.ac.jp

■ ACKNOWLEDGMENT

The work at Kyoto was supported by Grants-in-Aid (Nos. 22245006 (A) and 20108001 “pi-Space”) for Scientific Research from MEXT. E.T. and Y.I. acknowledge JSPS Fellowship for Young Scientists. This work at Seoul was supported by the Star Faculty and World Class University (R32-2009-000-10217-0), Programs of the Ministry of Education, Science and Technology (MEST) of Korea, and an AFSOR/AOARD Grant (FA2386-09-1-4092) (D.K.).

■ REFERENCES

- (1) (a) Clayton, R. K.; Sistrom, W. R., Eds. *The Photosynthetic Bacteria*; Plenum Press: New York and London, 1978. (b) Govindjee *Light Emission by Plants and Bacteria*; Ames, J., Fork, D. C., Eds.; Academic Press: New York and London, 1986. (c) Grondelle, R. V.; Dekker, J. P.; Gillbro, T.; Sundström, V. *Biochim. Biophys. Acta* **1994**, *1187*.
- (2) (a) Murphy, M. J.; Siegel, L. M.; Tove, S. R.; Kamin, H. *Proc. Natl. Acad. Sci. U.S.A.* **1974**, *71*, 612. (b) Roth, J. R.; Lawrence, J. G.; Bobik, T. A. *Annu. Rev. Microbiol.* **1996**, *50*, 137.
- (3) (a) Montforts, F. P.; Ofner, S.; Rasetti, V.; Eschenmoser, A.; Woggon, W. D.; Jones, K.; Battersby, A. R. *Angew. Chem., Int. Ed. Engl.* **1979**, *18*, 675. (b) Chang, C. K. *Biochemistry* **1980**, *19*, 1971. (c) Chang, C. K.; Hanson, L. K.; Richardson, P. F.; Young, R.; Fajer, J. *Proc. Natl. Acad. Sci. U.S.A.* **1981**, *78*, 2652. (d) Kim, H.-J.; Lindsey, J. S. *J. Org. Chem.* **2005**, *70*, 5475. (e) Ruzié, C.; Krayner, M.; Balasubramanian, T.; Lindsey, J. S. *J. Org. Chem.* **2008**, *73*, 5806. (f) Borbas, K. E.; Ruzié, C.; Lindsey, J. S. *Org. Lett.* **2008**, *10*, 1931. (g) Krayner, M.; Ptaszek, N.; Kim, H.-J.; Meneely, K. R.; Fan, D.; Secor, K.; Lindsey, J. S. *J. Org. Chem.* **2010**, *75*, 1016.
- (4) (a) Inokuma, Y.; Kwon, J. H.; Ahn, T. K.; Yoon, M.-C.; Kim, D.; Osuka, A. *Angew. Chem., Int. Ed.* **2006**, *45*, 961. (b) Kobayashi, N.; Takeuchi, Y.; Matsuda, A. *Angew. Chem., Int. Ed.* **2007**, *46*, 758. (c) Torres, T. *Angew. Chem., Int. Ed.* **2006**, *45*, 2834.
- (5) (a) Myśluborski, R.; Latos-Grażyński, L.; Sztrenberg, L.; Lis, T. *Angew. Chem., Int. Ed.* **2006**, *45*, 3670. (b) Kim, K. S.; Lim, J. M.; Myśluborski, R.; Pawlicki, M.; Latos-Grażyński, L.; Kim, D. *J. Phys. Chem. Lett.* **2011**, *2*, 477. (c) Xue, Z.-L.; Shen, Z.; Mack, J.; Kuzuhara, D.; Yamada, H.; Okujima, T.; Ono, N.; You, X.-Z.; Kobayashi, N. *J. Am. Chem. Soc.* **2008**, *130*, 16478.
- (6) (a) Inokuma, Y.; Yoon, Z. S.; Kim, D.; Osuka, A. *J. Am. Chem. Soc.* **2007**, *129*, 4747. (b) Inokuma, Y.; Easwaramoorthi, S.; Yoon, S.; Kim, D.; Osuka, A. *J. Am. Chem. Soc.* **2008**, *130*, 12234. (c) Inokuma, Y.; Easwaramoorthi, S.; Jang, S. Y.; Kim, K. S.; Kim, D.; Osuka, A. *Angew. Chem., Int. Ed.* **2008**, *47*, 4840. (d) Hayashi, S.; Inokuma, Y.; Osuka, A. *Org. Lett.* **2010**, *12*, 4148.
- (7) Tsurumaki, E.; Saito, S.; Kim, K. S.; Lim, J. M.; Inokuma, Y.; Kim, D.; Osuka, A. *J. Am. Chem. Soc.* **2008**, *130*, 438.
- (8) 14π -Aromatic compounds involving an unshared electron pair of nitrogen atom, see: (a) Anastassiou, A. G.; Elliott, R. L. *J. Am. Chem. Soc.* **1974**, *96*, 5257. (b) Fozard, A.; Bradsher, C. K. *J. Org. Chem.* **1967**, *32*, 2966.
- (9) Hayashi, S.; Inokuma, Y.; Easwaramoorthi, S.; Kim, K. S.; Kim, D.; Osuka, A. *Angew. Chem., Int. Ed.* **2010**, *49*, 321.
- (10) Spectroscopic data of **3d**; see Figure S4 of SI. At the present time, we isolated almost pure **3d** but failed its complete purification.
- (11) For the full Gaussian citation, see SI.
- (12) Crystallographic data for **3a-OEt**: $2(\text{C}_{35}\text{H}_{30}\text{B}_1\text{N}_3\text{O}_1) \cdot \text{C}_2\text{H}_5\text{N}$, $M = 1079.91$, monoclinic, space group $P2_1$ (no. 4), $a = 12.251(4) \text{ \AA}$, $b = 18.924(6) \text{ \AA}$, $c = 13.226(5) \text{ \AA}$, $\beta = 115.098(12)^\circ$, $V = 2776.9(16) \text{ \AA}^3$, $T = 123 \text{ K}$, $\rho_{\text{calcd}} = 1.292 \text{ g cm}^{-3}$, $Z = 2$, $R_1 = 0.0631$ ($I > 2\sigma(I)$), $R_w = 0.1840$ (all data), $\text{GOF} = 1.016$. CCDC-806996.
- (13) (a) Keegan, J. D.; Stolzenberg, A. M.; Lu, Y.-C.; Linder, R. E.; Barth, G.; Moscovitz, A.; Bunnenberg, E.; Djerassi, C. *J. Am. Chem. Soc.* **1982**, *104*, 4305. (b) Burkhalter, F. A.; Meister, E. C.; Wild, U. P. *J. Phys. Chem.* **1987**, *91*, 3228.
- (14) Gouterman, M. *J. Mol. Spectrosc.* **1961**, *6*, 138.